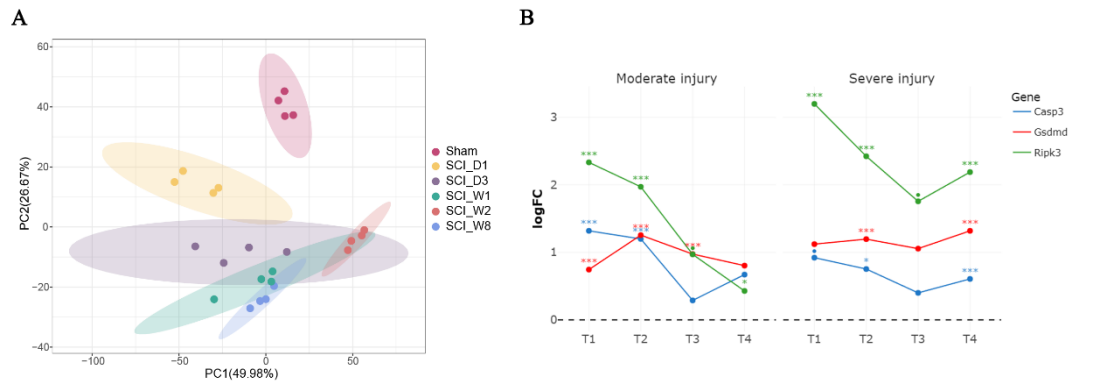


Figure S1: Temporal dynamics of gene expression and PCD pathway activation after SCI revealed by bulk RNA-seq.

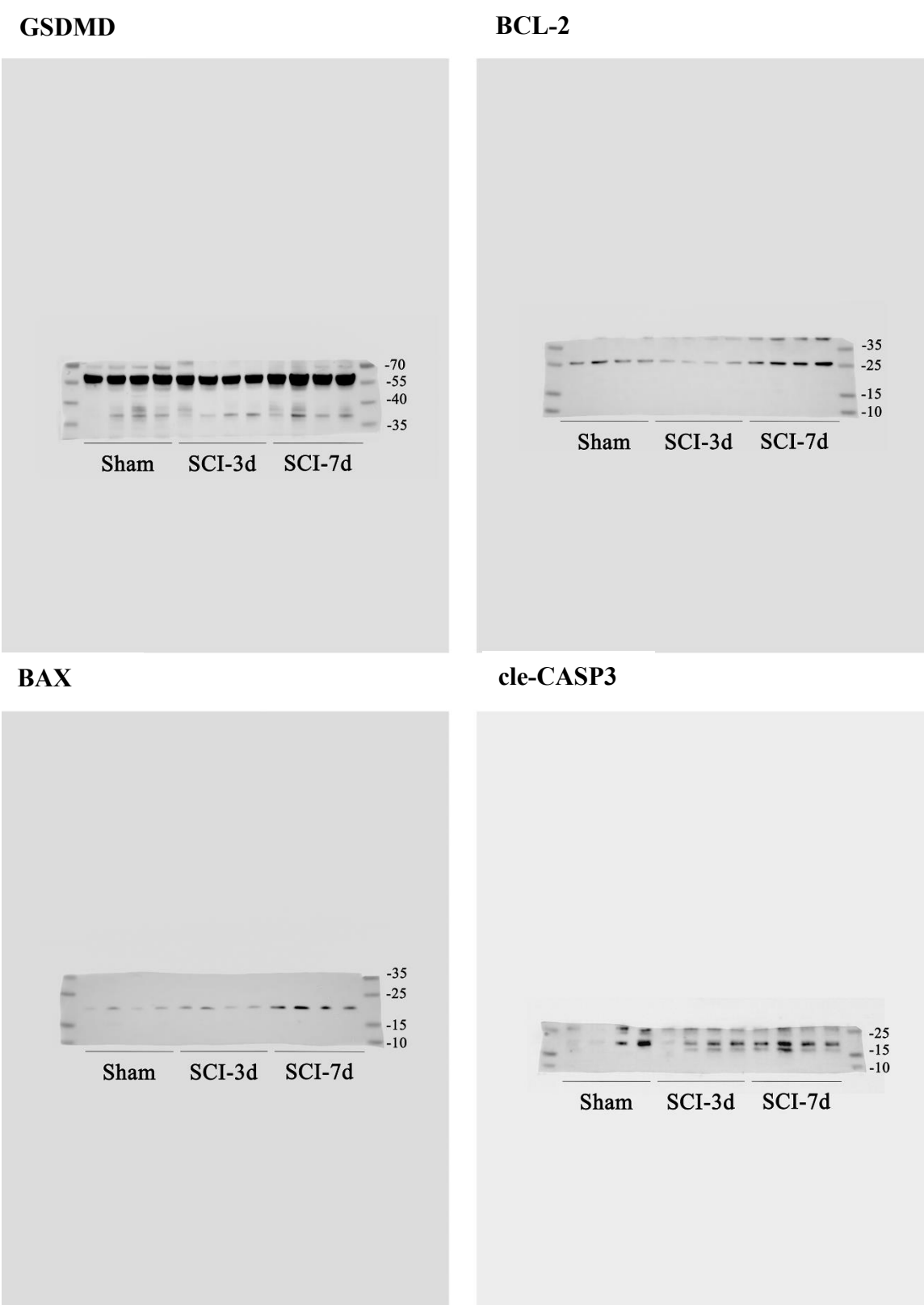


(A) PCA plot showing temporal clustering of spinal cord samples across different stages of spinal cord injury (SCI), indicating progressive transcriptomic changes.

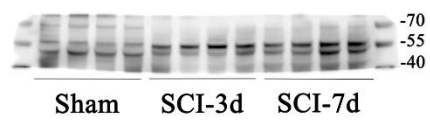
(B) Time-course expression profiles of core cell death executioner genes (*Casp3*, *Gsdmd*, *Ripk3*) in the meta-SCI database. T1, acute phase (0-3 days after SCI); T2, subacute phase (4-14 days after SCI); T3, early chronic phase (15-35 days after SCI); T4, late chronic phase (> 35 days after SCI).

• , p<0.1; *, p<0.05; ***, p<0.001.

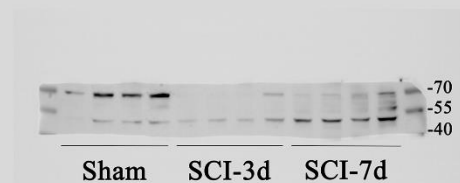
Figure S2: Corresponding uncropped full-length gels and blots in Figure 1I.



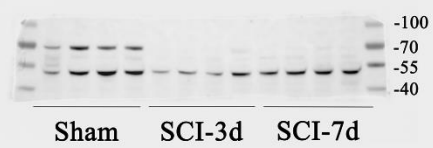
RIPK3



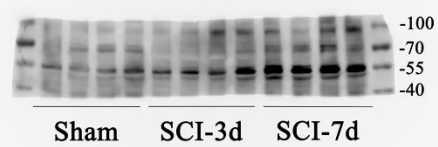
p-RIPK3



MLKL



p-MLKL



β -actin

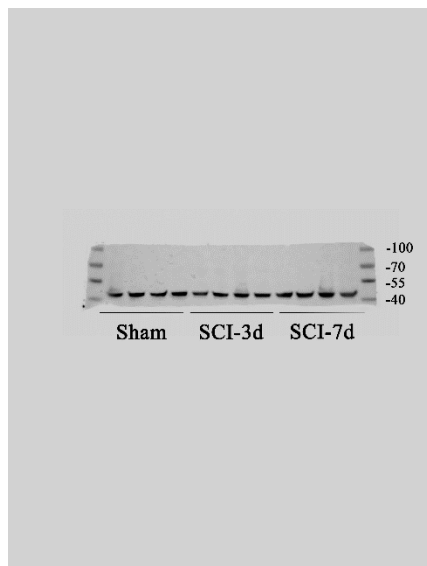
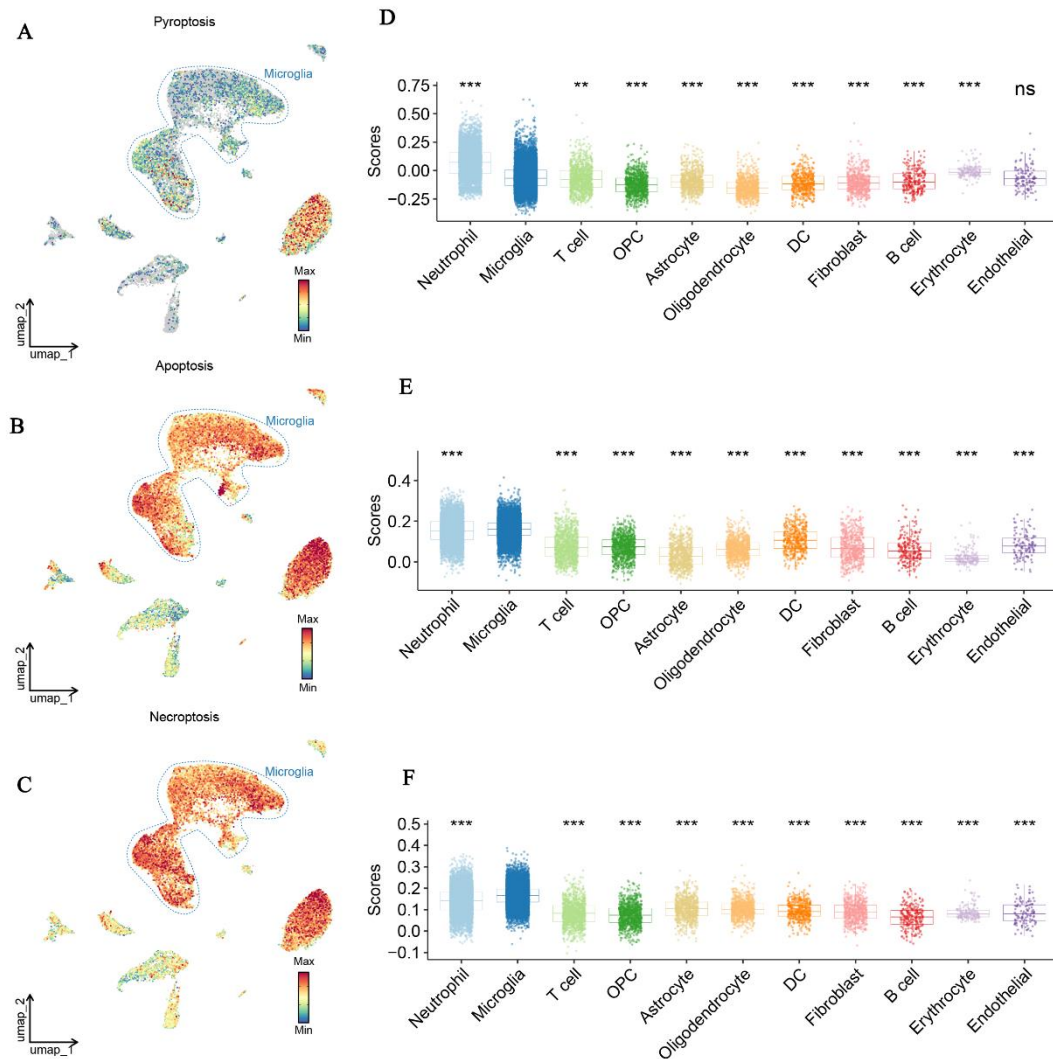


Figure S3: Microglia underwent pyroptosis, apoptosis, and necroptosis after SCI.

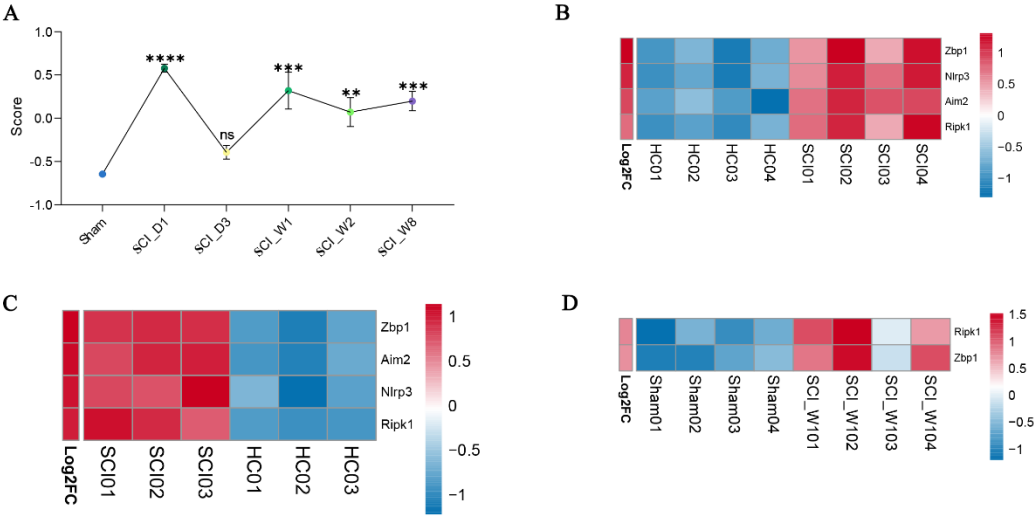


(A-C) UMAP visualization of pyroptosis (A), apoptosis (B), and necroptosis (C) pathways in all cell types using AddmoduleScore.

(D-F) Boxplots showing the pyroptosis (D), apoptosis (E), and necroptosis (F) pathway scores across cell types.

In (D-F), the box boundaries represent the 25th -75th percentiles; the midline indicates the median. Statistical significance was determined using the Kruskal-Wallis test with Dunn's post-hoc test: ns, non-significant; **, $p < 0.01$; ***, $p < 0.001$.

Figure S4: Bulk RNA-seq and scRNA-seq revealed the existence of PANoptosis in SCI rats.

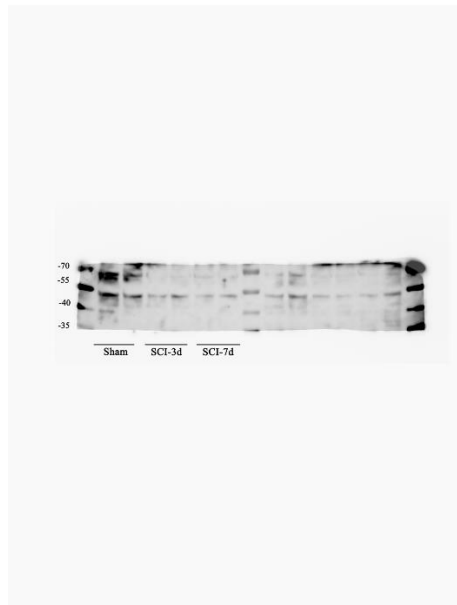


(A) Line chart showing dynamic change in PANoptosis activity across SCI stages, based on ssGSEA.

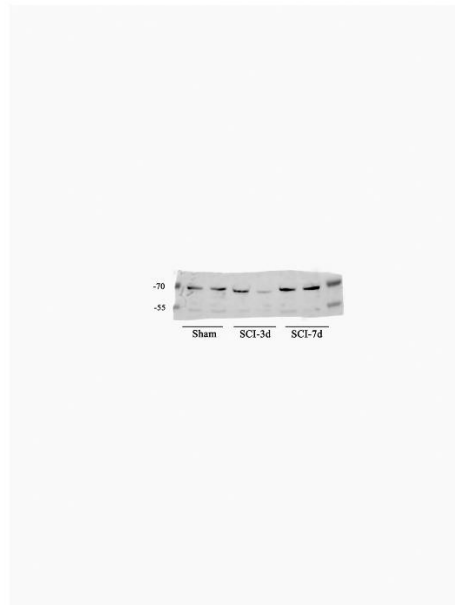
(B-D) Heatmap showing the expression of PANoptosis sensor at transcriptomic levels. ns, non-significant; **, $p<0.01$; ***, $p<0.001$; ****, $p<0.0001$.

Figure S5: Corresponding uncropped full-length gels and blots in Figure 3C.

AIM2



ZBP1



Vinculin

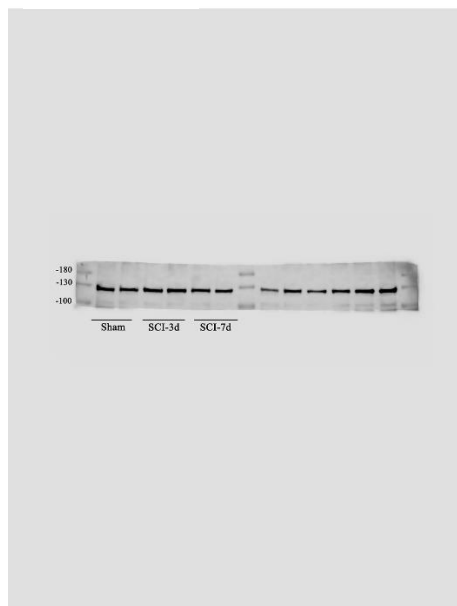


Figure S6: Dotplot showing the expression level of PANoptosome-related genes in all cell types.

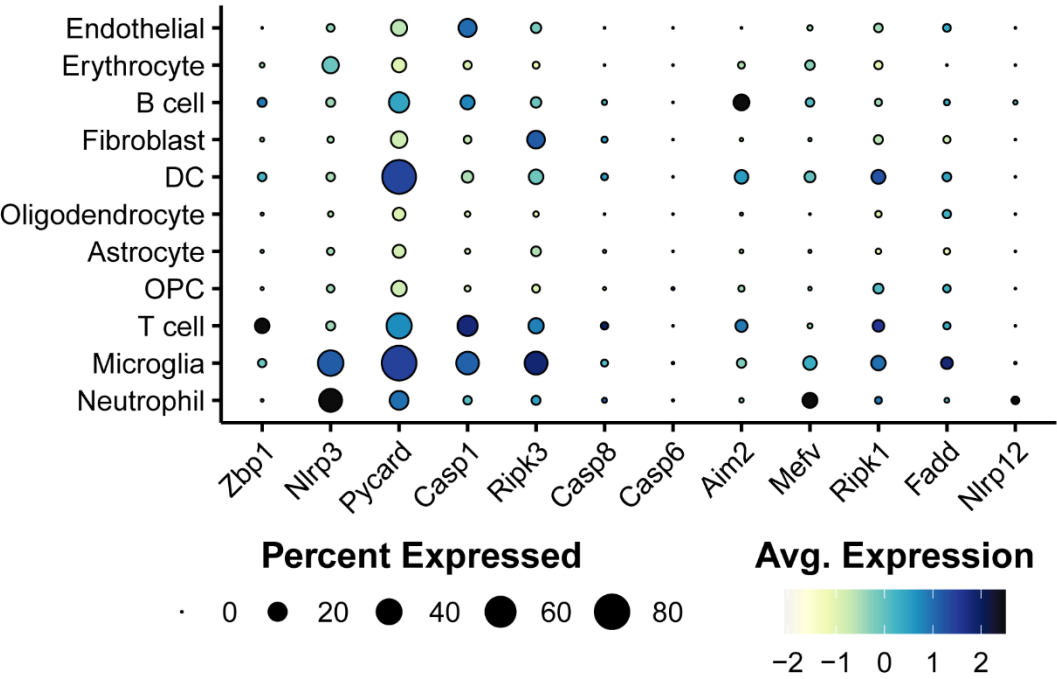
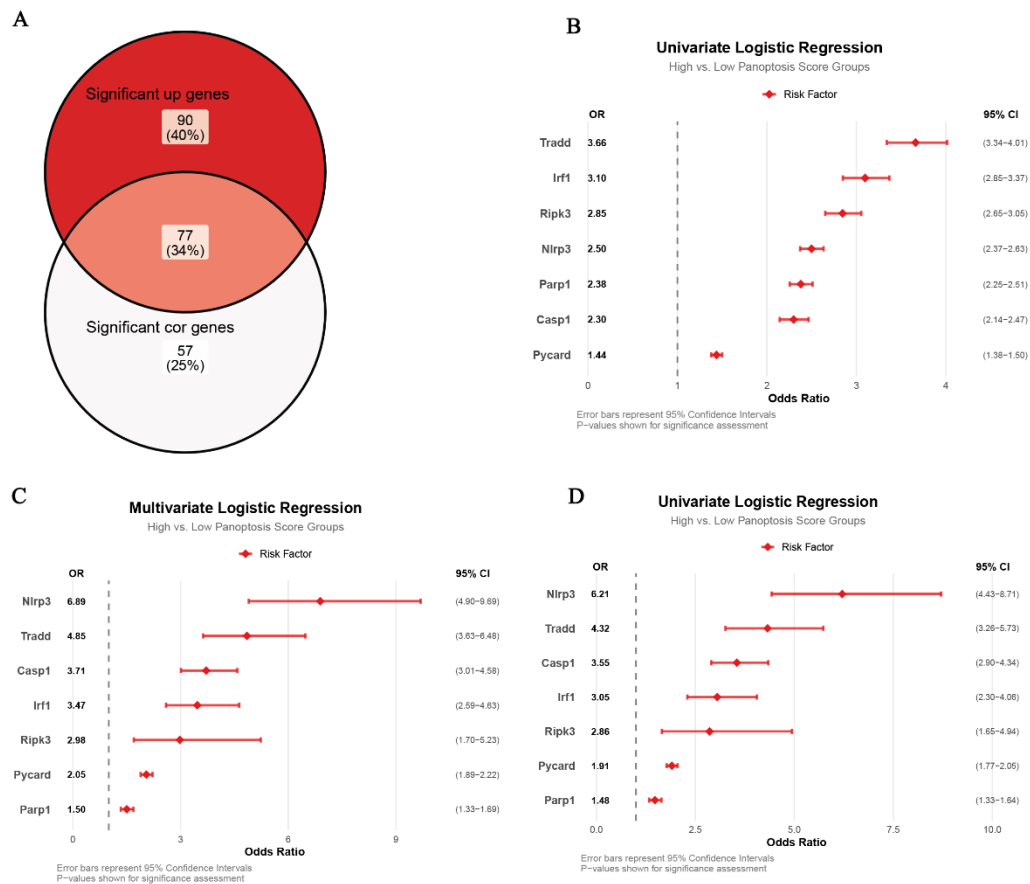


Figure S7: *Irf1* serves as an independent risk factor for PANoptosis in microglia.



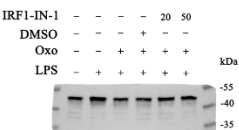
(A) Venn diagram showing the overlap between differentially expressed genes (DEGs) significantly upregulated in association with PANoptosis activity scores and genes significantly correlated with those scores.

(B) Forest plot displaying the OR and 95% CI from univariate logistic regression analysis.

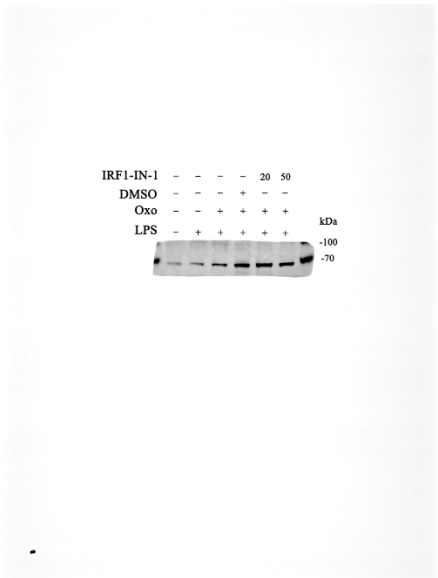
(C-D) Forest plots showing the results of multivariate (C) and univariate (D) logistic regression analyses based on scRNA-seq data from SCI mouse models.

Figure S8: Corresponding uncropped full-length gels and blots in Figure 5H.

IRF1



ZBP1



Vinculin

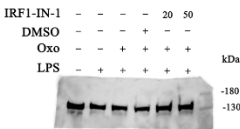
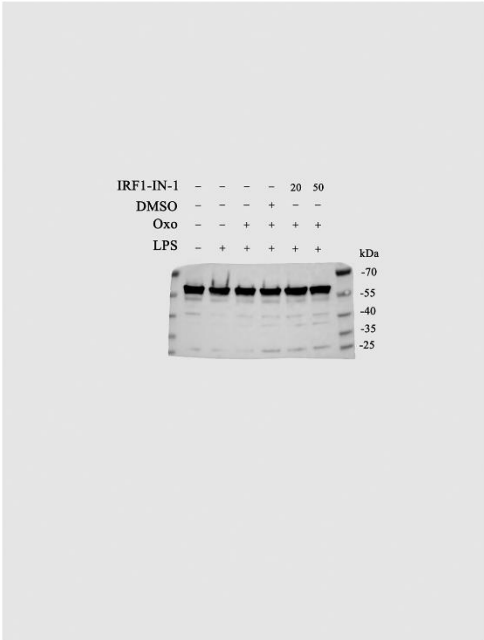
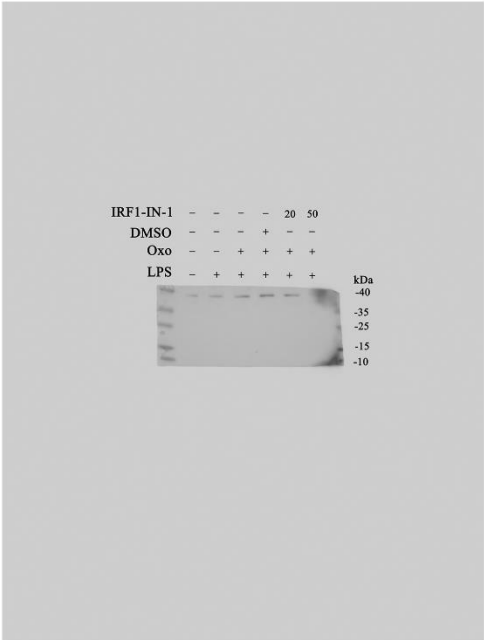


Figure S9: Corresponding uncropped full-length gels and blots in Figure 6B-C.

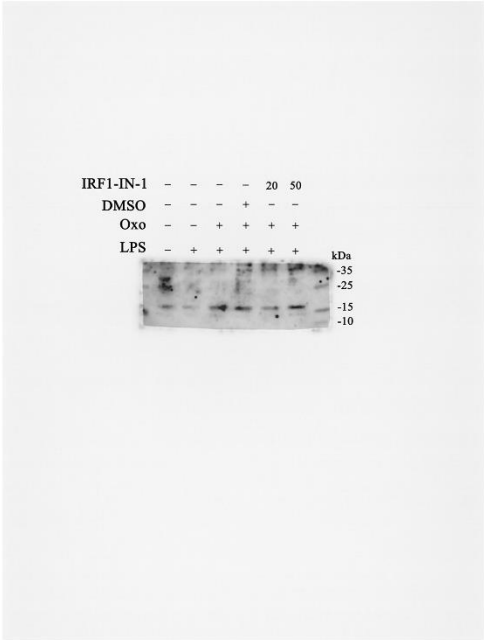
GSDMD



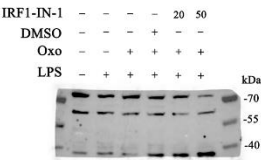
N-GSDMD



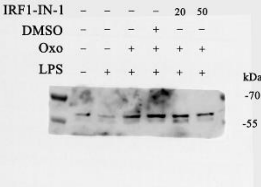
cle-CASP3



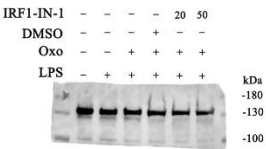
MLKL



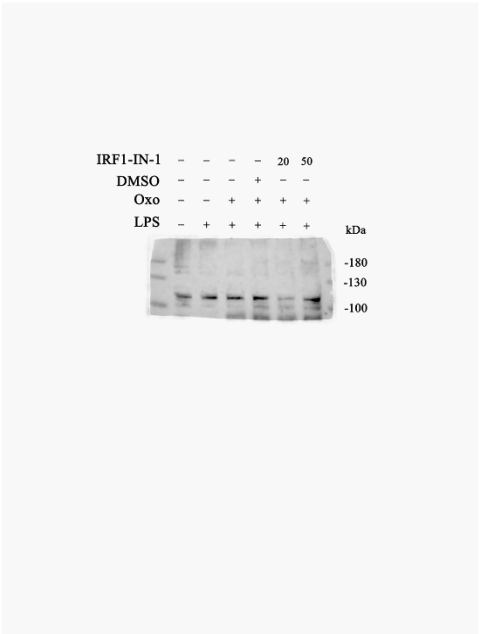
p-MLKL



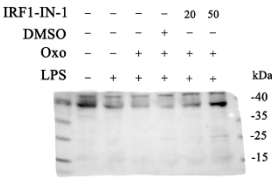
Vinculin



iNOS



Arg1



Vinculin

